International Journal of Engineering and Advanced Technology (IJEAT)
ISSN: 2249-8958 (Online), Volume-6 Issue-4, April 2017

Robust Analysis with Controller Design of Forward-Velocity Dynamics of UAVs in Close Formation Flight

Johnson Y, Imthias Ahamed T P

Abstract: ***Study of multi-UAVs (Unmanned Aerospace Vehicles) in close formation flight has received wide attention due to the significant advantages in resource mapping at greater swaths, 3-D imaging etc. The control design study and its analysis is carried out for two aerodynamically non-identical UAVs in a leader-follower pattern of flight and it can be extended for multi UAVs. The modeling includes the effect of leader-trailing-wing vortex on the follower, both for nominal and perturbed system dynamics. Robust controller design to maintain the relative velocity between two UAVs in longitudinal plane close formation flight under nominal, wind and aero-perturbed condition is the major objective of this article. The forward velocity control of the leading vehicle and its tracking by a follower are performed by a PID controller and then compared with that of a robust H_∞ controller.***

Keywords: Formation flight, UAV, PID, robust H-infinity, tracking and control, wing vortex.

I. INTRODUCTION

The application domain of Unmanned Aerospace Vehicles (UAVs) has extended from reconnaissance to scientific data collection in academic research. Multi UAVs in close formation flight can enhance its ability to collect data more efficiently. A formation flight problem in longitudinal plane focuses on the tracking issues of longitudinal states of forward velocity, distance, angle of attack and the pitch dynamics etc. of the leader vehicle in a leader-follower system. Among all the above states, the state which mainly focused on this paper is the forward velocity. Here the modification of the induced drag component on the follower dynamics due to the wing vortex effect of the leader is also taken for the proposed controller design and analysis. When the leader vehicle is subjected to heavy atmospheric wind effects in its flight, simultaneous perturbations may pass over to the follower dynamics. Unlike a conventional PID controller, a robust controller can maintain the control and tracking with negligible error even in the presence of external perturbations. This paper is organized as follows. After a brief literature review (section-II), the mathematical modeling of UAV close formation dynamics is presented (section-III). The simulation and the analysis of trailing wing vortex effect of the leader upon follower under nominal, Wind and aero-perturbed conditions through the leader-follower aerodynamics cross coupling is also discussed. Section-IV describes the control and tracking of leader dynamics using PID and robust H_∞ controllers, design of weights in H_∞ controller, the robust stability and performance analysis of leader and follower forward velocity dynamics under various atmospheric conditions such as nominal and perturbed, with respect to pole-zero diagrams, followed by some concluding remarks (section-V).

Manuscript published on 30 April 2017.
***** Correspondence Author (s)
Johnson Y*, PhD Research Scholar, Department of Electronics and Electrical Engineering, University of Kerala, Thiruvananthapuram (Kerala)-695034, India. E-mail: j_yoEannan2000@yahoo.com
Imthias Ahamed T P, Department of Electronics and Electrical Engineering, Thangal Kunju Musaliar College of Engineering, Kollam (Kerala)-691005, India.

II. RELATED WORKS

Several studies have been done in the flight control of UAVs. The most important among them are constraint forces approach [1], 3D potential field approach [2], intelligent management control approach [3], co-operative control [4, 5], vision based scheme [6] and constrained adaptive back stepping approach [7]. There are several tracking control schemes available in literature. Proud, A. et al. had done formation control on two aircrafts using PID feedback [8]. Vanek and Balint introduced practical approach to real-time trajectory tracking of UAV formations using model predictive control [9]. Saffarian and Fahimi present a modified leader-follower framework for achieving the formation and propose a model predictive nonlinear control algorithm [10]. A novel decentralized control design procedure is developed by Haibo Min which guarantees obstacle avoidance and collision [11]. Dogan et al. applied non linear control approach [12] for formation reconfiguration.

The major beneficial effect of the close formation flight is the induced drag reduction. Lot of studies have been reported dealing with drag reduction approach. C. F. Chichka, J. L. Spaeyer, C. Fanti and C. G. Park conducted a vast study about peak seeking control for drag reduction in formation flight [13]. Drag reduction in extended formation flight [14], simulation of aerodynamics cross-coupling vortex effects [15], computational aerodynamics of flexible wings for MAV [16], formation flight with greatest fuel savings benefits for the trail aircraft [17] are some of the significant studies dealing with wing vortex effects. The effect of heavy wind (more than 10m/s) upon vehicles during flight faces a challenging problem in modeling. The simulation of wind effects with flight data analysis has been done in [18]. The studies referred above do not establish robustness to large parameter uncertainties that are associated with such vehicles.

All these studies are suffered from the lack of computational efficiency and easiness in the controller design approach. In this paper, the existing robust control toolboxes in MATLAB.

Are appropriately utilized to solve these multidimensional problems and hence reduce the controller design complexities in the existing literature.

III. UAV CLOSE FORMATION MODELING BASED ON AERODYNAMIC COUPLING

The UAV in flight creates spiral like disturbances in its vicinity. The cylindrically shaped spiral disturbances are projected backward perpendicular to its wings on two sides. The air moves in a circular pattern in these disturbance pockets originating from the wing tips, enlarging the circles and dissipate over time gradually. Another disturbance effect is seen parallel to the wings moving up circularly towards UAV body. This disturbance phenomenon is called horseshoe vortex. The air movement between the vertical disturbances at the two wing tips is downwash whereas in the outside vicinity of horseshoe vortex, it is a combination of sidewash and upwash. The aerodynamic interaction between the vehicles in CFF affects the total flight behaviour. The reduction in the induced drag on follower occurs when it took advantage of the upwash effect from the wings of the leader. This is the advantage that a typical CFF system demands. The upwash and sidewash of the air vortex from leader wing tips affect the flight profile of follower. The required fuel that drives follower in-formation is less as compared to single flight.

A. Close Formation Modeling

The upwash effect produces reduced drag on follower. The corresponding longitudinal stability derivatives of the follower are proportionately affected. A.W. Proud had elaborated and derived the aerodynamic close formation effects quantitatively on a typical leader-follower system [19]. Some important equations useful for the present analysis are taken from [19] and are described in the following paragraphs.

The approximated wing span of the follower for an elliptical lift distribution on a wing using horseshoe vortex approach is $b' = \frac{\pi}{4}b$. The symbol b' is the effective wing span. The average induced upwash due to leader's vortices from both disturbance filaments originating from the leader's wings is,

$$W_{uw} = \frac{\Gamma_l}{4\pi b}\left(\ln\left[\frac{y_1^2+z_1^2+\mu^2}{(y_1-\pi/4)^2+z_1^2+\mu^2}\right] - \ln\left[\frac{(y_1-\pi/4)^2+z_1^2+\mu^2}{y_1^2+z_1^2+\mu^2}\right]\right)$$

here μ^2 is the correction factor to account for the physical viscosity effects and Γ_l is the vortex strength of leader wing tips which is given by $\Gamma_l = \frac{2C_{Ll}V_l b_l}{\pi AR_l}$ Where b_l - leader wing span; AR_l - leader aspect ratio; C_{Ll} - leader lift coefficient; V_l - leader velocity. The formation velocity of the system is assumed as leader velocity in subsequent analysis. If C_{Ll} value is not given, it is calculated

by $C_{Ll} = C_{L0l} + C_{L\alpha l}\alpha + C_{Lql}\frac{\bar{c}}{2V_l}q + C_{L\delta el}\delta e$

$y_1 = \frac{\bar{y}}{b}$ and $z_1 = \frac{\bar{z}}{b}$ are named as the non-dimensional formation geometry parameters. Here, $\bar{y}$ and $\bar{z}$ are the relative distances in lateral and vertical directions respectively between the vehicles. The value of y_1 is $\frac{\pi}{4}$ since $\bar{y}$ is taken as b' for achieving optimal drag reduction formation geometry and the value of $\bar{z}$ is taken as one-tenth of $\bar{y}$.

The change in follower angle of attack due to upwash is

$$\Delta\propto_f = \tan^{-1}\frac{W_{uw}}{V_l}$$

The drag on follower is changed due to the lift vector

rotation $\Delta D_f = L_f \tan\Delta\alpha_f$ $\qquad L_f = qS_f C_{Lf}$

(S_f - follower wing area; C_{Lf} - lift coefficient of follower, L_f- lift on follower wings). Drag during Formation Flight (DFF) is the difference between the induced drag and its incremental change due to formation. $D_{ff} = D_f - \Delta D_f$ $D_f = qS_f C_{Df}$ (C_{Df} - drag coefficient (for follower). When $''C_{Df}''$ is treated in close formation, it is defined by a new term, C_{Dff}.

$C_{Dff} = \frac{D_{ff}}{qS_f} = C_{Lf}\frac{W_{uw}}{V_l}$ The incremental change in non-dimensional drag coefficient $\Delta C_{Df} = C_{Df} - C_{Dff}$

The incremental change in the non-dimensional lift

coefficient $\Delta C_{Lf} = C_{L\alpha_f}\Delta\alpha$ $\qquad C_{Lff} = C_{Lf} + \Delta C_{Lf}$

Where C_{Lff} is the value of C_{Lf} when UAVs are in formation. Both lift and drag effects are taken for the determination of new stability coefficients, even though relative change in lift is very small compared to that of drag. Moreover, since $L >> D$, drag is influenced by the rotation effect significantly than lift.

B. Longitudinal Simulation and its Analysis

The flight profile simulation of the proposed formation flight system is done in two phases: nominal and perturbed. In nominal phase, externally applied disturbances are completely absent which is an ideal case. But the induced wing vortex effects from the leader are taken care of. Perturbed phase is more like a real situation in which a limited range of change is applied in the values of some selected longitudinal or lateral stability and control derivatives. The selection of stability derivatives is based on their sensitivity or response to a particular open loop follower plant dynamics WVU YF-22 aircraft is taken as the leader & CONDOR HE-UAV as the follower for the present simulation. The geometrical and aerodynamic data for leader and follower are taken from references [20] and [21] respectively. The follower UAV, namely, Condor Hybrid Electric (HE) aircraft was designed and constructed by a Colorado-based UAV design firm named CL Max Engineering.

Published By:
Blue Eyes Intelligence Engineering
and Sciences Publication (BEIESP)

The wings are of Eppler 210 airfoil configuration while its tail is configured with NACA 0009 airfoil. Due to modeling limitations, the NACA 2412.

Airfoil was substituted in place of the Eppler 210 since the performance difference between the two is insignificant. The follower aerodynamic stability and control derivatives are estimated and are given in Table-II [20, 21]. Its developed controllers and other related accessories are not considered for this academic simulation. The nominal aerodynamic profile given in terms of state space data is performed at straight and level flight.

The longitudinal dynamics equation for a single UAV in state-space form portrays the multivariable coupling among longitudinal states of forward velocity(u),angle of attack(α), pitch rate(q) and pitch angle(θ) with two inputs[22]. The terms are explained in Table-VII. For the leader, only one input, i.e, the stabilator (elevator), is used and the corresponding data in steady and level conditions is given. For the follower, both elevator and throttle are used together having MIMO dynamics structure and its numerical data is also given.

$$\begin{bmatrix}\dot{u}\\ \dot{\propto}\\ \dot{q}\\ \dot{\theta}\end{bmatrix}=\begin{bmatrix}X_u & X_\alpha & X_q & X_\theta\\ Z_u & Z_\alpha & Z_q & Z_\theta\\ M_u & M_\alpha & M_q & M_\theta\\ 0 & 0 & 1 & 0\end{bmatrix}\begin{bmatrix}u\\ \alpha\\ q\\ \theta\end{bmatrix}+\begin{bmatrix}X_{\delta i_1} & X_{\delta i_2}\\ Z_{\delta i_1} & Z_{\delta i_2}\\ M_{\delta i_1} & M_{\delta i_2}\\ 0 & 0\end{bmatrix}\begin{bmatrix}\delta i_1\\ \delta i_2\end{bmatrix}$$

$$\begin{bmatrix}\dot{u_l}\\ \dot{\alpha_l}\\ \dot{q_l}\\ \dot{\theta_l}\end{bmatrix}=\begin{bmatrix}-0.2835 & -23.0959 & 0.00 & -0.17\\ 0.00 & -4.1172 & 0.7781 & 0.00\\ 0.00 & -33.8836 & -3.5729 & 0.00\\ 0.00 & 0.00 & 1.00 & 0.00\end{bmatrix}\begin{bmatrix}u_l\\ \propto_l\\ q_l\\ \theta_l\end{bmatrix}+\begin{bmatrix}20.168\\ 0.5435\\ -39.08\\ 0.00\end{bmatrix}[\delta_s]$$

$$\begin{bmatrix}\dot{u_{f1}}\\ \dot{w_{f1}}\\ \dot{q_{f1}}\\ \dot{\theta_{f1}}\end{bmatrix}=\begin{bmatrix}-0.047 & -0.039 & 0 & -32.2\\ -0.374 & -4.592 & 50.8 & 0\\ 0.0015 & -0.7248 & -2.62 & 0\\ 0 & 0 & 1 & 0\end{bmatrix}\begin{bmatrix}u_{f1}\\ w_{f1}\\ q_{f1}\\ \theta_{f1}\end{bmatrix}+\begin{bmatrix}0 & 0.15\\ -35.7 & 0\\ -66.1 & 0\\ 0 & 0\end{bmatrix}\begin{bmatrix}\delta_e\\ \delta_\tau\end{bmatrix}$$

The follower longitudinal dynamics data contains dimensional stability and control derivatives. These derivatives are functions of dynamic pressure which by themselves are functions of both local atmospheric density (altitude) and velocity. The given follower CONDOR HE-UAV undergoes a steady level flight of velocity 17m/s at a height of 366m. When it enters into formation with the leader which flies steadily with 42m/s velocity at a level of 120m above ground, two factors are used to modify the present data in order to achieve close formation mechanism with dependent aerodynamic interactions. One is the ratio of two velocities and the other one is the ratio of local atmospheric densities. The density ratio is very small as compared to the velocity ratio and can assume to be neglected in practical considerations. All the other non-dimensional stability and control derivatives and geometric parameters like mass, wing area, chord length etc. will not undergo any variations in these transformations. The transformed [A] and [B] matrices of the follower at the leader height and speed level are:

$$A=\begin{bmatrix}-0.11 & -0.09 & 0 & -32.2\\ -0.87 & -10.7 & 118.36 & 0\\ 0.0035 & -1.69 & -6.12 & 0\\ 0 & 0 & 1 & 0\end{bmatrix};\ B=\begin{bmatrix}0 & 0.815\\ -193.6 & 0\\ -358.98 & 0\\ 0 & 0\end{bmatrix}$$

(i). Nominal Aerodynamic Profile

The available and estimated parameters given in Table-III & IV are used to find the following aerodynamic quantities using the formulae described in the beginning of this session. These numerical calculations are crucial for understanding the aerodynamic interaction between the vehicles and the controller design in the following simulation.

The calculated quantities under nominal conditions are:

lift coefficient of leader, $C_{Ll}=0.118$; vortex strength, Γ_l =2.38 m^2/s ; average induced upwash, W_{uw}=0.08; change in AOA, $\Delta\propto_f$ = 0.11 deg; follower lift, L_f = 1803.6 N; change in drag, ΔD_f = 3.43 N; drag, D_f =18 N; the Drag during Formation Flight (DFF), D_{ff} = 14.6 N; change in lift, ΔL_f = 0.0342 ; the Lift during Formation Flight (LFF), L_{ff} = 1803.63 N; modified drag coefficient of follower by vortex effect, $C_{Dff}=0.01$.

The achieved reduction in drag, as per calculation, is 20%. Thus the calculated modified drag coefficient of follower is from the upwash wing vortex effects since the upwash is responsible for the angle of attack (AOA) variation of follower's wings.

(ii) Perturbed Aerodynamic Profile

The perturbations considered for the present simulation are (a) the atmospheric wind and (b) the variation in aerodynamic derivatives or coefficients.

Effect of Wind

The flight trajectory and the longitudinal stability derivatives of the UAV dynamics are changed due to its effect. The wind magnitude is limited to 5m/s. The effective velocity contains the wind component. Assume that wind flows in the same direction of UAVs. The effective velocity is the summation of two quantities since the wind is assumed to have no lateral components. The aerodynamic parameters which depend on velocity are changed. The calculated values of variables under perturbation are (the suffix 'p' in the notations of variables represent perturbed values):

$V_{lp}=47m/s$; Γ_{lp} = 2.67 $\frac{m^2}{s}$; W_{uwp} = 0.09; $\Delta\propto_{fp}$ = 0.109 deg ; L_{fp} = 2258.6 N; ΔD_{fp} = 4.3 N;
$D_{fp}=22.58N$; $D_{ffp}=18.28N$; ΔL_{fp} = 0.043 N; L_{ffp} = 2258.64 N; C_{Dffp}=0.0105.

The velocity induced dynamic pressure variations have no effect in the leader lift coefficient since the value of the term C_{Lql} is zero in this case. So the relative changes in lift characteristics due to the velocity increment are very small compared to drag effects.

Effect of changes in aero coefficients

Variations in aerodynamic stability derivatives usually occur during flight from their pre-flight estimated values. It may occur either in leader or follower dynamics or both. As a typical case study, consider a typical follower longitudinal forward velocity dynamics with elevator input plant, $\frac{u}{\delta e}$. From fig.3, The most sensitive three parameters in order are $C_{m\propto}$, $C_{m\delta e}$ and C_{Lq}.

Published By:
Blue Eyes Intelligence Engineering
and Sciences Publication (BEIESP)

IV. CONTROLLER DESIGN AND ITS ANALYSIS

The controllability and observability of the system matrices are checked and it is assured that the system

is both controllable as well as observable. The evaluation of control and tracking characteristics can be done better by considering the required specifications either in time or frequency domain. The step response specifications in time domain desirable to the performance analysis are given in Table-III. The first option selected for this moment is the classical PID controller since it is known for well damped response with minimum errors and its design simplicity.

A. PID Controller

The classical PID controllers are used at first to control various states of leader and follower dynamics independently and to track the leader states accurately under nominal and perturbed conditions. If the results got with PID are not satisfied with the required specifications, some other control action having more robustness can be used instead for the same purpose. PID parameter tuning is performed with optimization technique. The closed loop unit step responses of PID controlled leader forward velocity dynamics plant under nominal and perturbed conditions are given in fig.1. With the parameter values of $k_p = -0.47$, $k_i = 0.43$ and $k_d = 0.09$, the achieved time response specifications for leader forward velocity control under nominal conditions are: rise time $(t_r) = 0.82$ sec; settling time $(t_s) = 1.8$ sec and overshoot = 8% . Its closed stability is also checked and found to be stable with a gain margin (GM) of 19.3@6.43 rad/s and a phase margin (PM) of 60@1.66 rad/s. So PID is enough to control the given leader forward velocity state in nominal conditions. But in one perturbed condition (with changing C_{Lq}), unbounded oscillations had resulted. In that case the stability of the system is checked and found to be unstable with GM of 35.61@12.2 rad/s and PM of -2.63@2.45 rad/s. So PID fails at this moment. It is noticed that the PID designed for nominal conditions is no longer able to maintain the performance and robustness requirements for the given perturbed conditions [24]. So some robust control techniques should be applied for getting precise solution.

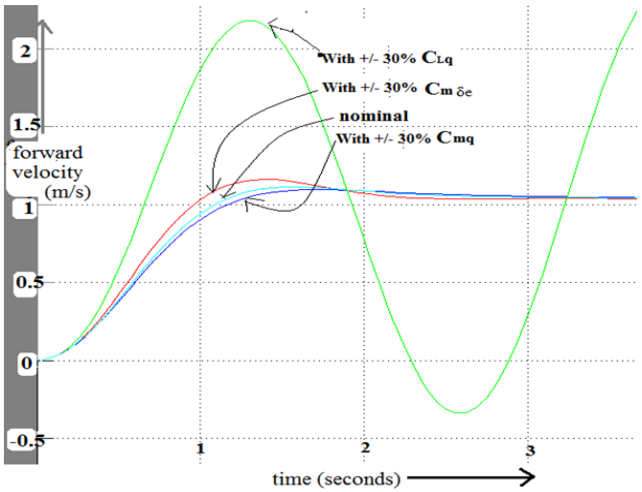

Fig.1: Unit Step Response of PID Controlled Leader Forward Velocity Dynamics Under Nominal and Perturbed Conditions.

Table. I Desired Step Response Specifications for Control and Tracking

Serial No	Time Domain Specifications	Value
1	Rise time	< 1 sec
2	% rise	90
3	Settling time	< 2 sec
4	% settling	3
5	% overshoot	10
6	% undershoot	2

Table II Geometrical Data of UAVs

Symbol	Quantity	Leader WVU YF-22	Follower CONDOR HE- UAV	Unit
B	Wing span	1.96	4	M
S	Wing area	1.37	1.3	m^2
AR	Aspect ratio	2.6	12	
$\bar{c}$	Mean aerodynamic chord	0.76	0.33	M
M	Mass	20.64	30 lb	Kg
V	Cruise speed	42	18	m/s
T	Thrust	54.62		N
α_{trim}	Angle of attack(trim)	3	0	Deg
θ_{trim}	Pitch angle(trim)	3		Deg
I_{xx}	Moment of Inertia (M.I.)about roll axis	1.6	3.884 $slug.ft^2$	kgm^2
I_{yy}	M.I. about pitch axis	7.51	1.572 $slug.ft^2$	kgm^2
I_{zz}	M.I. about yaw axis	7.18	4.569 $slug.ft^2$	kgm^2
H	Height	120		M

TABLE-II Longitudinal Stability Derivatives

Symbol	Leader	Follower	Unit
$C_{m\alpha}$	-0.473	-1.6219	$^1/_{rad}$
$C_{m\dot{\alpha}}$	-3.9142	-3.91416	$^1/_{rad}$
C_{mq}	-3.449	-11.7426	
C_{mu}	0.022	0	
$C_{m\delta e}$	-0.364	-2.93565	$^1/_{rad}$
C_{lu}	-0.001		
$C_{l\beta}$	-0.038		
$C_{L\alpha}$	3.258	6.0508	$^1/_{rad}$
C_{Lq}	0		$^1/_{rad}$
$C_{L\delta e}$	0.189		$^1/_{rad}$
$C_{L\delta f}$		0.69	
C_{Lu}	-0.049	0.055862	$^1/_{rad}$
$C_{D\alpha}$	0.508	0.271383	$^1/_{rad}$
C_{Du}	0.008	0	$^1/_{rad}$
C_{Dq}	0	0	
$C_{D\delta e}$	-0.034		$^1/_{deg}$

Published By:
Blue Eyes Intelligence Engineering
and Sciences Publication (BEIESP)

B. H_∞ Controller

The basic object in H_∞ control is a stable and proper transfer function. H_∞ denotes the space of bounded analytic functions in the open Right Half Plane (RHP). H_∞ controller helps to select a transfer function with least H_∞ norm. In graphical perspective, it is actually the minimization of the peak in bode magnitude plots. Examples are the Sensitivity function, S(s) and the Complementary sensitivity function, T(s). Unlike the classical LQG control which minimizes the closed loop peak for known input signals, H∞ control deals with unknown inputs, resulting in 'flat' Bode magnitude plots. Loop-shaping techniques are used to impose particular shapes to the output responses.

The given H_∞ control problem is formulated to find a robust controller for the generalized plant such that $\infty-$norm of the transfer function relating d to z is minimum. The robust H_∞ controller is chosen for the control and tracking because it can maintain stability not only in nominal plants, but for real plants also [25]. A H_∞ controlled plant with appropriate frequency dependent weights is shown as a block diagram in fig.6. The transfer functions of plant and weights should be proper and stable, otherwise the stabilizability conditions of augmented matrix (plant transfer function with weights) along with the gain will not be satisfied. The weights are designated as W1, W2 and W3. W1, known as sensitivity weight or performance weight, penalizes the error signals. The control weight W2 penalizes the control signal. The output signal is penalized by complementary sensitivity weight or stability weight W3.

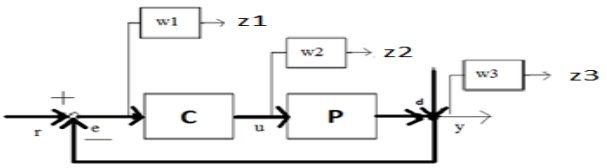

[C–controller; P–plant;r - reference;e – error;u – plant input;y – actual output;z1 – desired error signal;z2 – desired input signal;z3 – desired output signal]

Fig.2: H_∞- Controlled Leader Tracking Dynamics Plant.

For multivariable (MIMO) transfer matrices, H_∞ norms are described with the concept of singular values.

The well known parameter selection rules for H_∞ control weights are reproduced below [26].

(a) For achieving better performance i.e. good disturbance rejection, design W1 such that it should be small inside desired control bandwidth. So it requires small value of sensitivity function (S) in low frequency region. Keep in mind that 1/W1 should have the general shape of 'S'. The sensitivity function S can be suitably shaped by properly designing the weighted norm $\|W1(s).S(s)\|_\infty$.

(b) In order to achieve good stability margin i.e. robustness, select W3 such that it should be small outside desired control bandwidth. So it requires small value of complementary sensitivity function (T) in high frequency region. The weight 1/W3 should have the general shape of 'T'. For robust stability requirement, the infinity norm of the weighted 'T' function should be equal or less than one, i.e., $\|W3(s).T(s)\|_\infty \leq 1$. Based on the design rules (a) & (b) above, the weights are designed such that the desired parameters have the following values for forward velocity state. ω (desired closed-loop bandwidth) : 90; M (desired bound on H_∞ norm): 1; A (desired disturbance attenuation inside bandwidth): $\frac{1}{1500}$(for leader velocity control),$\frac{1}{1706}$ (for follower velocity control) and $\frac{1}{510}$ (for leader velocity tracking)

The Sensitivity (S) & Complementary sensitivity (T) functions for tracking forward velocity dynamics (under perturbation with 70% of $C_{m\delta e}$value) are shown graphically as Singular Value (SV) plots in fig.3. The shape of S and T verified the rules regarding its required shape.

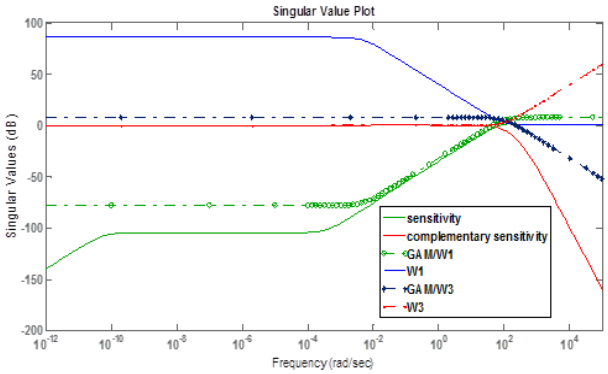

Fig. 3: Singular Value plot showing S & T.

The leader and follower output responses obtained in various conditions with the help of newly designed H_∞ controllers are given in figures from fig.4 to fig.6. The forward velocity of the leader UAV is controlled within less than 0.1 seconds as shown in the top part of fig.4. When the simulation is repeated with 30% change in the parameter C_{Lq} in the forward velocity plant transfer function, only 0.02 seconds is delayed in its control in the perturbed state from the nominal one. In the follower forward velocity control simulation, the time delays of only 0.01 and 0.03 seconds can be noticed with 30% change in $C_{m\delta e}$ and C_{Lq} parameters respectively in the forward velocity transfer function. An enlarged view of a small section of the top part of fig.4 is given in fig.5. This leader forward velocity in nominal conditions can be successfully tracked by a perturbed follower UAV with a small time delay of 0.02 sec, as shown in fig.6.

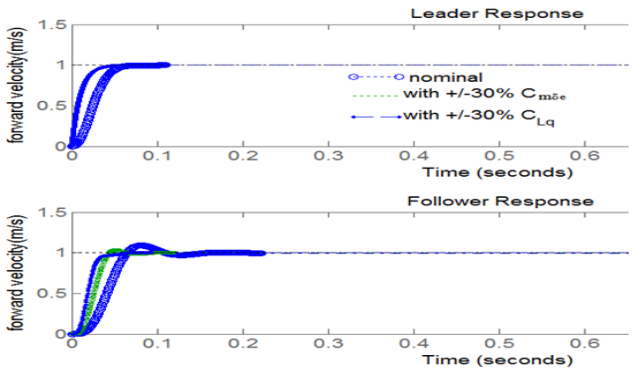

Fig.4: Unit step response of (a) leader (top) and (b) follower (bottom) H_∞ controlled forward velocity dynamics under various conditions

Published By:
Blue Eyes Intelligence Engineering
and Sciences Publication (BEIESP)

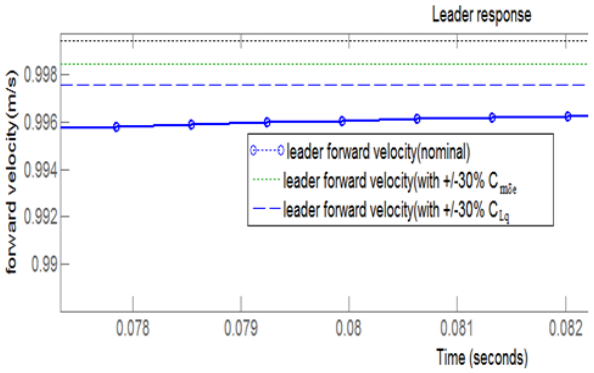

Fig.5: Enlarged view of a small section of top part of Fig.4.

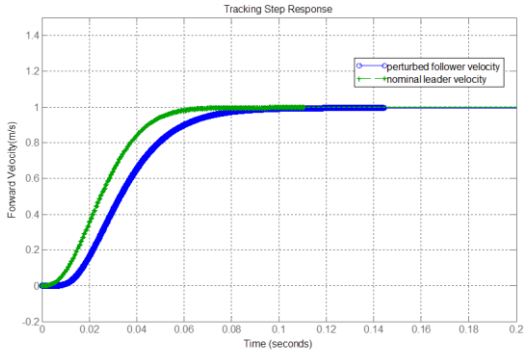

Fig.6: Unit step response of leader nominal forward velocity and its tracking by follower under perturbed condition.

Table IV: The Comparative Study

Sett ling time	Forward-velocity	Leader	Nominal	PID	1.8 s
				H_∞	0.1 s
			Perturbed	PID	∞
				H_∞	0.12s
		Follower	Nominal	PID	1.9 s
				H_∞	0.1 s
			Perturbed	PID	∞
				H_∞	0.13 s
		Tracking follower	Nominal	PID	1.9 s
				H_∞	0.09 s
			Perturbed	PID	∞
				H_∞	0.12 s

C. Comparative Study and the Stability Analysis

The comparative stability analysis of the overall system dynamics will help to get better concepts about system stability and control. The performance comparison can be done by comparing the responses in fig.1 and fig 4(a) along with fig.5 in terms of the settling time behaviour in the time domain characteristics of the leader forward velocity trajectories in nominal and perturbed (30% change in C_{Lq}) conditions with PID and H_∞ controllers. The leader with PID in closed loop requires 1.8 seconds to settle its forward velocity step response which is within the specified time of 2 seconds. But in 30% C_{Lq} condition the unstable unbounded oscillations did not lead to proper settling. H_∞ controlled leader requires only 0.1 second to settle in nominal conditions as compared to 1.8 seconds of the PID counterpart. But in the perturbed conditions H_∞ produces astonishing performance with settling time of only 0.12 second against the unbounded unstable behaviour with the PID counterpart. In the case of follower similar results had occurred. With the development of tracking H_∞ controller the perturbed follower advances by 0.01 second in its tracking of the leader compared to the case of without tracking controller. The comparative study detailed above is summarized in Table-IV.

V. CONCLUSION

The close formation flight UAV system consists of two aerodynamically non-identical UAVs. Their longitudinal stability and control derivatives are determined from the flight profile and geometric data. The trailing wing vortex effect of the leader upon follower dynamics under nominal and wind and aero-perturbed conditions are numerically calculated. The forward velocity dynamics is particularly focused and their individual control and tracking issues are tuned with a conventional PID and robust H_∞ controllers and their performance are compared. The robustness property of H_∞ at the cost of high control input is also revealed.

REFERENCE

1. Zou, Y. and Pagilla, P.R., "Distributed Formation Flight Control Using Constrained Forces", J. of Guidance, Control and Dynamics, Vol.32, No.1, 2009
2. Paul, T., Krogstad, T.R. and Gravdahl, J.T., 'Modeling of UAV Formation Flight Using 3D Potential Field', Simulation Modeling Practice and Theory,Vol.16, Issue 9,pp.1453-1462,2008
3. Innocenti, M., Guilietti, F. and Pollini, L., 'Intelligent Management Control for Unmanned Aircraft Navigation and Formation keeping', RTO AVT Course at Belgium, May, 2002
4. How, J., King, E. and Kuwata, Y., 'Flight Demonstration of Cooperative control for UAV Teams', AIAA 3rd Unmanned Unlimited Technical Conference, Workshop and Exhibit, Illinois, 2004
5. Yoon S., Bae. J, and Kim. Y, Cooperative Standoff Tracking of a Moving Target using Decentralized Extended Information Filter, KSAS (Korean Society for Aeronautical and Space Science) Spring Conference, Gyeongju, Republic of Korea, Apr 2011
6. Kim H.J., Kim. M, Lim. H, Park. C, Yoon. S, Lee. D, Oh. G, Park. J and Kim. Y, 'Fully-Autonomous Vision- based Net-Recovery Landing System for a Fixed-Wing UAV',IEEE/ASME Transactions on Mechatronics, accepted for publication, 2013.
7. S. Yoon, S. Park, and Y. Kim, 'Constrained Adaptive Backstepping Controller Design for Aircraft Landing in Wind Disturbance and Actuator Stuck',International Journal of Aeronautical and Space Sciences, Vol. 13, No. 1, pp. 101-116, 2012.
8. Proud, A., Pachter, M., and DAzzo, J. J., 'Close Formation Control', Proceedings of the AIAA Guidance, Navigation, and Control Conference, AIAA - 99 – 4207, pp. 123 1 - 1246, Portland, OR, August, 1999.
9. Vanek and Balint, 'Practical approach to real-time trajectory tracking Of UAV formations' ,Proceedings of the American Control Conference,2005.
10. Saffarian, M. and Fahimi, F., 'Control of helicopters formation using non-iterative nonlinear model predictive approach, Proceedings of IEEE American Control Conference, pp. 3707-3712, Seattle, Washington, June 2008
11. Min,H., Decentralized UAV formation tracking flight control using gyroscopic force, IEEE International Conference on Computational Intelligence, 2009.
12. Dogan,A. and Venkataramanan,S., 'Nonlinear control for Reconfiguration of Unmanned Aerial Vehicle Formation', J. of Guidance, Control and Dynamics, Vol 28, No 4(2005)
13. Chichka D.F.,Speyer J.L.,Fanti C. and Park C.G., Peak-seeking Control for Drag Reduction in Formation Flight, AIAA Journal of Guidance, Control and Dynamics,University of California,2002.
14. Ning S.A., Aircraft Drag Reduction through Extended Formation Flight,PhD thesis,Dept of Aeronautics and Astronautics,Stanford University, August 2011.

Published By:
Blue Eyes Intelligence Engineering and Sciences Publication (BEIESP)

15. Saban,D.,Whidborne,J.F. and Cooke A., Simulation of Wake Vortex Effects for UAV in close formation flight, Aeronautical Journal, Volume 113, Issue 1149,pp. 727-738,2009.
16. Shyy,W.,Lian Y.,Tang J.,Liu H.,Trizila P.,Stanford P.,Bernal L.,Cesnik C.,Freedmann P. and Ifju P., Computational Aerodynamics of Low Reynolds Number Plunging, Pitching and Flexible Wings for MAV Applications, Proceedings of the 46th AIAA Aerospace Sciences Meeting and Exhibit 7 - 10 January 2008.
17. Morgan M.T., A Study in Drag Reduction of Close Formation Flight accounting for trim control flight positions and Dissimilar Formations. ,thesis,M.S.Aeronautical Engineering,Air force Institute of Technology, March,2005.
18. Lewis T.A., Flight Data Analysis and Simulation of Wind Effects during Aerial Refuelling. ,thesis, M.S. Aerospace Engineering, University of Texas,Arlington,May,2008.
19. Proud, A.W., "Close Formation Flight Control", M.S. Thesis in Electrical Engineering, Air Force Institute of Technology, Air University, March, 1999.
20. Campa,G,Gu,Y.,Design and Flight Testing of Non-linear Formation Control Law,Science Direct,Control Engineering Practise 15,pp-1077- 1092,2007.
21. Christopher G., "Modeling, Simulation and Flight test for Automatic Flight Control of the Condor Hybrid-Electric Remote Piloted Aircraft," Thesis, M.S. Aeronautical Engineering, Presented to the faculty, Departments of System Engineering, Aeronautics and Astronautics, Air University, March, 2012
22. Nelson, R.C., "Flight Stability and Automatic Control", Tata McGraw-Hill Publishing Company Ltd., New Delhi, 2nd edition, 2007.
23. Johnson Y. and Dasgupta S., "Robust Hurwitz Stability and Performance Analysis of H-Infinity Controlled Forward-Velocity Dynamics of UAVs in Close Formation Flight Using Bounded Phase Conditions in a Kharitonov Framework', Int. J. Inst. Eng. India, Springer Publications, Series. C, vol 95, Issue 3, pp 223-231, July 2014.
24. Johnson Y. and Dasgupta S., "Control and Tracking of Longitudinal Dynamics of UAVs in Synchronized Motion," Conference Proceedings, IEEE, International Conference on Control Communication and Computing (ICCC), Trivandrum, 2013
25. Scherer C., "Theory of Robust Control", Delft University of Technology, The Netherlands, April 2001
26. Johnson Y. and Dasgupta S., "Pitch Attitude Dynamics Control and Tracking of UAVs in Close Formation Flight," Int. Conf. on Emerging Trends in Electrial Engineering (ICETREE-14), Kollam, Kerala, India, Conference Proceedings, Elsevier Publications, 2014.

Published By:
Blue Eyes Intelligence Engineering
and Sciences Publication (BEIESP)